



Modeling topographic influences on fuel moisture and fire danger in complex terrain to improve wildland fire management decision support

Zachary A. Holden^{a,*}, W. Matt Jolly^b

^a US Forest Service, 200 East Broadway, Missoula, MT 59807, USA

^b US Forest Service Rocky Mountain Research Station, Fire Sciences Laboratory, Missoula, MT 59808, USA

ARTICLE INFO

Article history:

Received 8 June 2011

Received in revised form 31 July 2011

Accepted 2 August 2011

Available online 14 September 2011

Keywords:

Wildfire danger

Climate

Weather

Topoclimate

Snowmelt

Microclimate

ABSTRACT

Fire danger rating systems commonly ignore fine scale, topographically-induced weather variations. These variations will likely create heterogeneous, landscape-scale fire danger conditions that have never been examined in detail. We modeled the evolution of fuel moistures and the Energy Release Component (ERC) from the US National Fire Danger Rating System across the 2009 fire season using very high resolution (30 m) surface air temperature, humidity and snow ablation date models developed from a network of inexpensive weather sensors. Snow ablation date occurred as much as 28 days later on North-facing slopes than on South-facing slopes at upper elevations. South-facing slopes were hotter and drier than North-facing slopes but slope position, in addition to aspect, was also important because nocturnal air temperatures were coolest and humidity was highest in valley bottoms. These factors created heterogeneous fuel moistures and fire danger across the study area. In the late season (August and September), nocturnal cold air drainage and high relative humidity fostered fuel moisture recovery in valley bottoms, where fuel moistures and ERC values were 30% and 45% higher and lower, respectively at peak fire danger (September 29th). Dry fuel moistures and relatively high ERC values persisted on low elevation, South-facing slopes. The driest conditions were observed 100–200 m above the valley floor where mid-slope thermal belts frequently developed above areas of cold air pooling. We suggest that a complete understanding of these variations may help improve fire management decision making.

Published by Elsevier B.V.

1. Introduction

Topography and weather interact in complex mountainous terrain to create steep biophysical gradients that are principally driven by changes in solar radiation and elevation. Solar insolation fosters warmer temperatures and greater surface energy exchange on exposed slopes and elevation influences daytime adiabatic lapse rates (Geiger, 1966). While some of the general patterns of air temperature variation in mountains are known, their interactions with other physical factors like snowmelt, climatic water balance and moisture content of dead woody debris have not been well characterized.

Wildland fire danger models use information about fuels and weather to estimate the potential that fire may ignite and spread in a particular area (Cohen and Deeming, 1985). These models use sensible weather parameters to estimate both fuel moisture content and certain indices that are related to the characteristics of an initiating fire such as the potential heat release, nominal rates of spread and flame lengths. These fuel moistures and indices are

used by fire managers to both plan for expected changes in fire potential before ignitions have occurred or to determine an appropriate response to a wildland fire once an ignition takes place.

The National Fire Danger Rating System (NFDRS) was designed to capture worst case conditions, with Remote Automated Weather Stations (RAWS) typically located at mid-elevation South-facing slopes (Cohen and Deeming, 1985). Subsequently, the fire danger ratings based on these worst case scenarios are applied across large areas. These weather stations tell us very little about the variability in fuel moistures in complex topography because they do not sample a range of terrain conditions. Variation in snowmelt timing, surface air temperatures and relative humidity and incident radiation are known to vary with topographic position but their influence on fine-scale spatial variation in fuel moisture and wildfire danger indices has not been examined. Improved characterization of spatial variation in fuel moisture and fire potential could be useful for fire managers tasked with making decisions about how best to manage wildfires or prioritize limited resources during the fire season.

The purpose of this study was to analyze the influences of fine-scale topoclimatic variation on fuel moistures and a common fire danger index across the 2009 fire season. We use inexpensive air

* Corresponding author. Tel.: +1 406 329 3119.

E-mail address: zaholden@fs.fed.us (Z.A. Holden).

temperature and relative humidity sensors to derive high spatial resolution daily surface air temperature, humidity and snowmelt timing data, predicted across a topographically complex landscape. We then use these data to estimate microclimate-corrected fuel moistures and fire danger across an example study area in Southwestern Montana, USA. We examine the evolution of fuel moistures and fire danger across the 2009 fire season in order to characterize the terrain-mediated variation in fuel moistures and fire danger across the landscape. We present a simple method that can be used to scale weather station derived-fire danger across a landscape while accounting for terrain induced reductions in fire danger. We suggest that a complete understanding of these variations may help improve fire management decision making.

2. Methods

2.1. Study area and data

This study was conducted in Skalkaho Basin in the Sapphire Mountains of the Bitterroot National Forest, Montana (Fig. 1). The authors and local wildland firefighters deployed a network of 140 temperature and 57 relative humidity sensors across the area in May, 2009. Sensors were hung on the North side of a tree at 2 m height in a pair of inverted funnels following [Hubbart et al. \(2005\)](#). More information about the sensors and study design is available in [Holden et al. \(2011\)](#). These sensors collected data continuously at 90 min intervals from 16 May–29 September, 2009.

Elevation and topographic data for this study came from a Digital Elevation Model (DEM) derived from Light Detection and Ranging (LiDAR) acquired in October, 2009. The 1 m DEM was extracted using the software package FUSION ([McGaughey, 2010](#)) and resampled to 30 m. Additional topographic indices used in the analysis (solar radiation and topographic dissection described later) were derived from the Advanced Spaceborne Thermal Emissions Radiometer (ASTER) topography mission ([Gillespie et al.,](#)

2005). This was necessary to account for topographic shading effects of mountains beyond the LiDAR acquisition area in the calculation of solar insolation.

Thirty-six air temperature sensors were installed approximately 1 cm below the ground surface around the Skalkaho Basin study area at random locations stratified by solar radiation and elevation. Data from these sensors was used to infer snow ablation date (SAD) at each site (Fig. S1). Topographic variables used to predict SAD included elevation, April–October cumulative solar radiation and topographic dissection ([Evans, 1972](#)) calculated using a 210×210 m window size. These were used as independent variables in an empirical model to predict SAD. Additional detail on these data and methods can be found in the [Supplementary materials](#).

Fire danger index calculations from the US National Fire Danger Rating System require estimates of temperature, relative humidity, sky cover and precipitation duration. Data from our microclimate network provides information about spatio-temporal changes in temperature and relative humidity. Precipitation and sky cover were not measured concurrently with temperature and relative humidity, therefore we assume that these values were consistent across the study area. These assumptions are detailed below. In this study, we focus on deriving spatially-explicit, daily temperature and humidity surfaces to inform our fire danger calculations. A complete description of the derivation of these key surface meteorology fields is given below.

2.2. Analysis methods

2.2.1. Snowmelt timing data and model

A simple algorithm was used to identify the last day where snow was present at each sensor (Fig. S1). We then developed an empirical General Additive Model (GAM; [Hastie and Tibshirani, 1990](#)) with Julian day of SAD as a response variable and topographic variables (elevation, solar radiation and topographic dissection) as predictors (Fig. S2). Detailed descriptions of the model methods and results are shown in the [Supplementary materials](#).

2.2.2. A PCA-based approach for modeling surface air temperature and humidity

Maps of daily predicted nocturnal minimum and maximum temperatures (T_{\min} , T_{\max}) and minimum and maximum relative humidity (RH_{\min} , RH_{\max}) were produced for our study area using the PCA-based downscaling approach described by [Holden et al. \(2011\)](#). Their analysis shows that PCA can be used to separate and then model the spatial (PC loadings) and temporal (PC scores) variability in temperatures from a network of inexpensive temperature sensors. The loadings (values corresponding to the location of each sensor) represent the weights of a data matrix after the scores are removed and are correlated with topographic indices derived from a DEM. The scores (one for each day) are correlated with daily weather observations from nearby RAWS stations. These scores and loadings can be separately modeled and then recombined to estimate the original values at new locations where no *in situ* data were available. A major limitation of the ibutton sensors for any near real-time application is that they must be retrieved before any analysis can be done and thus only provide retrospective data. By independently modeling the spatial and temporal variation among a network temporary ibutton sensors, we create empirical algorithms that can be used to later predict fine-scale topoclimatic variation after the sensors have been retrieved and are no longer available. Importantly, this method simultaneously captures the daily spatio-temporal variation in temperatures, which vary with atmospheric conditions (e.g. relative humidity and atmospheric pressure). [Holden et al. \(2011\)](#) describe the application of this approach for modeling minimum temperatures and cold air drainage.

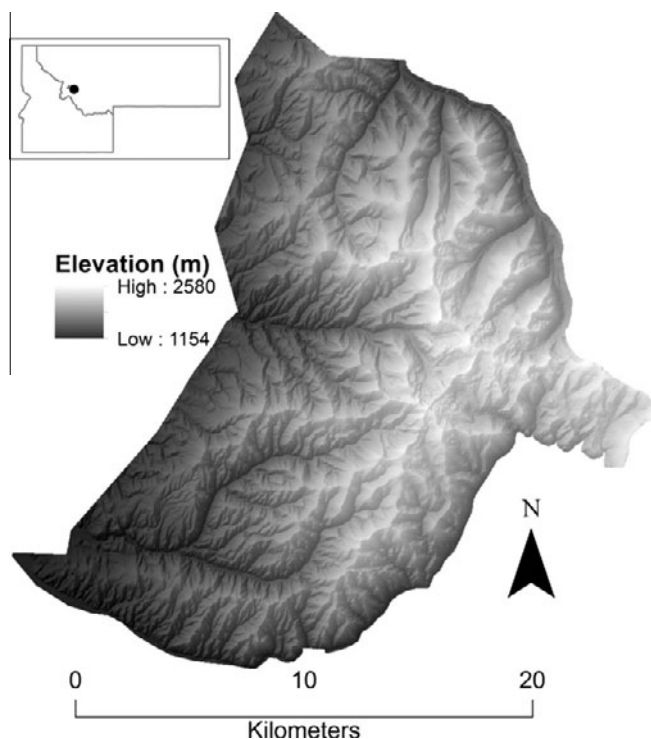


Fig. 1. Digital elevation model of the study area and Skalkaho Basin LiDAR acquisition area draped over a 10 m hillshade.

In this study, we adapt their approach to model maximum temperatures and relative humidity.

2.2.3. Surface air temperature downscaling

Maps of daily predicted nocturnal minimum temperatures (T_{\min}) were produced for our study area using models described by Holden et al. (2011). We used the same Principal Components Analysis method to empirically model daily spatial and temporal variation in maximum temperatures (T_{\max}). A more detailed description of the methods used to model T_{\max} is provided in the Supplementary methods.

2.2.4. Relative humidity downscaling

Twenty-five relative humidity sensors located nearest to the center of our study area were used to model spatial variation in relative humidity. PC loadings from minimum (daytime) RH were fit to elevation and solar radiation grids from a digital elevation model. PC loadings from maximum (nighttime) humidity were fit to elevation and a multi-scale dissection index (MSD) described by Holden et al. (2011). MSD is an index of relative cell position derived from a moving window calculation on a DEM, and calculated across multiple window sizes. This index was previously found to be strongly correlated with patterns of cold air drainage. Daily weather data were obtained from the Gird Point RAWs station (hereafter referred to as GP) that falls within the study area and PC time series were fit to temperature, relative humidity and solar radiation observations from that station.

2.2.5. Fuel moisture and fire danger index calculations

Fuel moistures (1, 10, 100 and 1000 h time lag classes) and a daily fire danger index (Energy Release Component – ERC) were calculated across the 2009 fire season at each 30 m grid cell using predicted snow melt timing, T_{\min} , T_{\max} , RH_{\min} and RH_{\max} as inputs to US National Fire Danger Rating System equations (Cohen and Deeming, 1985). Following recommendations from Andrews et al. (2003) the same fuel model (fuel model G) was applied to all pixels across the landscape. Using a single fuel model ensures consistent and comparable fire danger calculations between grid cells. Live fuel moistures were assumed to remain constant during the study and were thus fixed at 100% for both woody and herbaceous fuels. However, this assumption does not affect our fire danger predictions because the fire danger estimates using fuel model G were not sensitive to changes in live fuel moisture. A sensitivity analysis where only live fuel moisture was varied only changed ERC by 1–2 points across a range of live fuel moistures from 30% to 300%. Because the primary focus of this study was to examine the influence of topoclimatic temperature and humidity variations on fire danger, and because we do not have information about precipitation heterogeneity across the landscape, the daily precipitation duration and state-of-the-weather (sky cover) for the study period from GP was applied equally across entire study area. Heavy dead fuels (100 and 1000 h) were assumed to begin drying on the date of predicted snow departure. Finally, the daily ERC for each grid cell was calculated following equations described by Cohen and Deeming (1985). Gridded daily Energy Release Components values were then normalized using the following equation:

Relative Fire Danger Index

$$= \left(\frac{\text{GridPointValue} - \text{GridMinimumValue}}{\text{GridMaximumValue} - \text{GridMinimumValue}} \right) * 100 \quad (1)$$

where *GridPointValue* is the spatially-explicit, calculated grid point ERC for a given day, *GridMinimumValue* is the minimum value observed across all grid points for that day and *GridMaximumValue* is the maximum value observed across all grid points for that day. The final metric is continuous and bounded between zero and

100, where zero indicates a pixel with the minimum fire danger for that day and 100 indicates a pixel where fire danger was maximum for that day. The resulting daily maps from this normalization depict spatial patterns of fire danger across the landscape for a given day. We examined shifts in the distribution of ERC values across the fire season by plotting density functions of average biweekly ERC values from July–September. Finally, ERC values calculated at GP were then used to rescale the daily gridded ERC values as follows:

$$\begin{aligned} \text{GridPointFinalValue} = \text{RFDI (RAWS ERC value)} \\ - \text{GridMinimumValue} \\ + \text{GridMinimumValue} \end{aligned} \quad (2)$$

where *GridPointFinalValue* is the rescaled Energy Release Component value, *RFDI* is the pixel-based, Relative Fire Danger Index from Eq. (1), *RAWS ERC value* is the daily ERC value calculated at the RAWs station that falls within the study area and *GridMinimumValue* is the daily minimum grid value as defined in Eq. (1).

3. Results

3.1. Variation in snow ablation date

The date of snow ablation was well explained by three topographic variables. A General Additive Model with elevation, solar radiation and topographic dissection (210 × 210 m window) as predictor variables had an r^2 of 0.77 and a Root Mean Squared Error of 6.9 days (Table S1). This model was predicted to a 30 m resolution topographic layers to produce raster grid of predicted Julian day of snow departure for 2009 (Fig. 2B). Snow departure date varied significantly with elevation and with aspect at upper elevations, with predicted snow departure occurring earliest on Southwest-facing slopes and as much as 28 days later on North-facing slopes than on South-facing slopes at the high elevation sites.

3.2. Variation in surface air temperature extremes

Predicted minimum air temperature models capture the daily variation in the magnitude of cold air drainage from night to night. Average minimum nighttime temperatures for the study area are shown in Fig. 2D. PCA on daily T_{\max} from 52 ibuttons yielded two principal components that explained 98% of the variation among ibuttons. PC loadings, representing the weight of each station after the PC extractions were correlated with elevation and April–October cumulative incident solar radiation (Fig. S5). Random forest models for PC1 and PC2 loadings explained 60% and 95% of the variation, respectively (Table 1). The overall RMSE using a 10% data withhold cross-validation run 100 times was 2.42 °C. Fig. 2C shows average maximum air temperatures across the study period. Predicted maximum temperatures were warmer on South-facing slopes and temperatures decreased with elevation (Fig. 3). Lapse rates vary significantly from day to day, ranging from 4 °C/1000 m on overcast days to 7.5 °C/1000 m on hot, dry days.

3.3. Variation in daily relative humidity extremes

PCA on daily minimum (daytime) relative humidity from 25 ibuttons yielded two principal components that explained 97% of the variation among ibuttons. PC1 and PC2 loadings, representing the weight of each station after the PC extraction were correlated with elevation and April–October solar radiation (Fig. 4). Random forest models for PC1 and PC2 loadings with elevation and solar radiation as independent variables were moderately strong, with pseudo- R^2 values (variance explained) of 61% and 62%, respec-

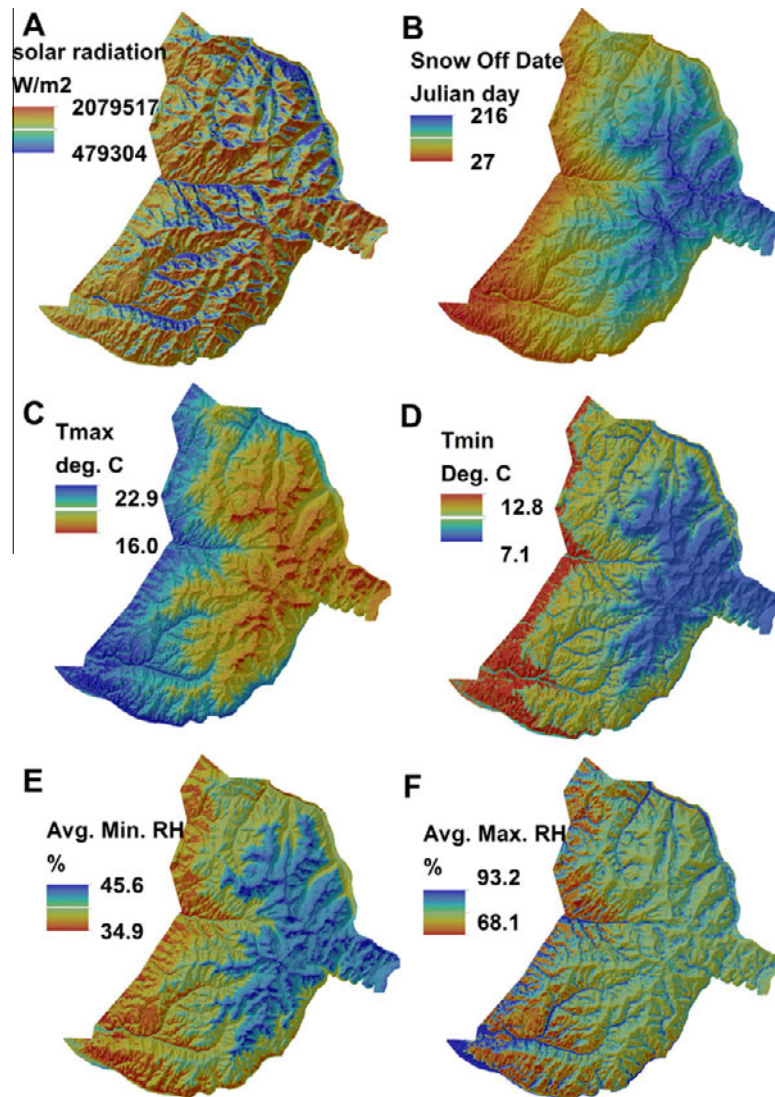


Fig. 2. Maps of total growing season solar radiation (A), snow ablation (off) date (B), mean maximum daily temperature (C), mean minimum daily temperature (D), mean minimum daily relative humidity (E) and mean maximum daily relative humidity(F). All means were calculated over the study period from 15 May–19 September, 2009.

Table 1
Accuracy results for models of PC loading for temperature and humidity models. Root Mean Squared Error (RMSE) results are based on a 10% data withhold performed 100 times.

Variable	# Sensors	PC1 load pseudo- R^2	PC2 load pseudo- R^2	Model RMSE
T_{\min}	52	0.64	0.95	1.47 °C
T_{\max}	52	0.58	0.81	2.42 °C
RH_{\min}	25	0.38	0.91	7.2%
RH_{\max}	25	0.49	0.95	13%

tively. PC scores were well correlated with minimum relative humidity and maximum temperature at the nearby GP station (Fig. 5). PC scores were applied back to predicted loading surfaces to create daily maps of RH_{\min} . Average RH_{\min} (15 May–29 September) is shown in Fig. 2E. Landscape patterns of RH_{\min} show drier South and west-facing slopes and decreasing humidity with increasing elevation (Fig. 6).

PCA on daily maximum relative humidity from 25 ibuttons yielded two principal components that explained 96% of the variation among ibuttons. PC1 and PC2 loadings, representing the weight of each station after PC extraction, were well correlated with elevation and a multi-scale dissection index (MSD) (Fig. 7). Random forest models for PC1 and PC2 loadings with elevation and MSD as independent variables were strong, with accuracies

of 62% and 68%, respectively (Table 1). PC scores on RH_{\max} were well correlated with maximum relative humidity and minimum temperature at GP (Fig. 8). Cross-validation using a 10% data withhold yielded a RMSE of 13% (Table 1). PC scores were applied back to predicted loading surfaces to create daily maps of RH_{\max} . Average RH_{\max} (15 May–29 September) is shown in Fig. 2F. RH_{\max} was highest in valley bottoms and on North- and East-facing slopes (Fig. 8).

3.4. Spatial variation in fuel moistures and ERC

Predicted fuel moistures and ERC showed large variability with terrain, and their spatial pattern changed throughout the fire season. Daily maps of normalized and predicted ERC values for 3 days

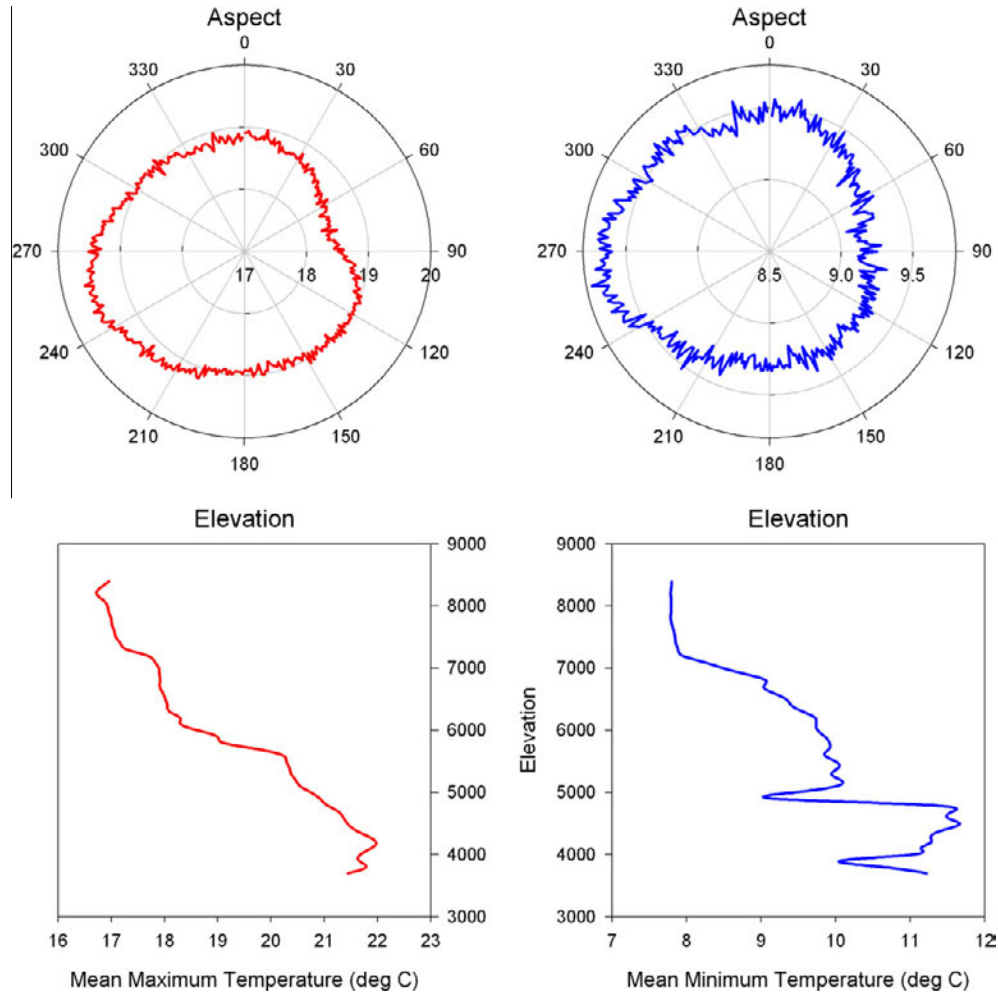


Fig. 3. Radial plots showing the distribution of predicted minimum and maximum temperatures by elevation and aspect.

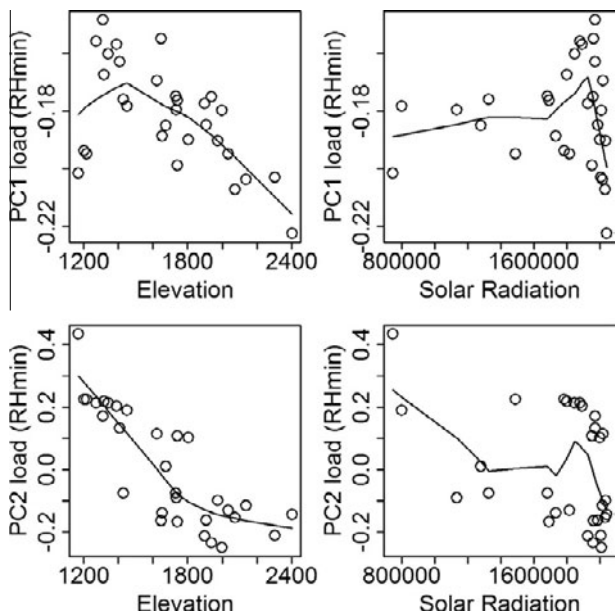


Fig. 4. Scatter plots and lowess smoothing curves showing relationships between PC loadings from minimum daytime relative humidity and elevation and solar radiation.

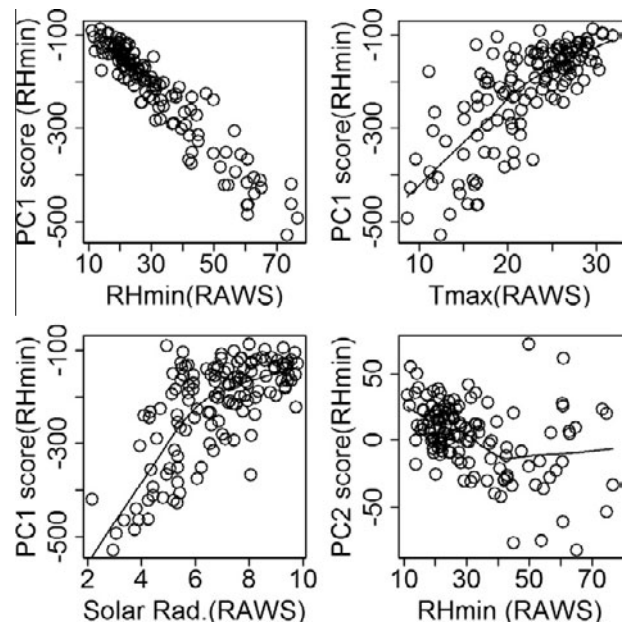


Fig. 5. Scatter plots and lowess smoothing curves showing relationships between PC loadings from minimum relative humidity and RAWS-observed minimum relative humidity, maximum temperature and solar radiation.

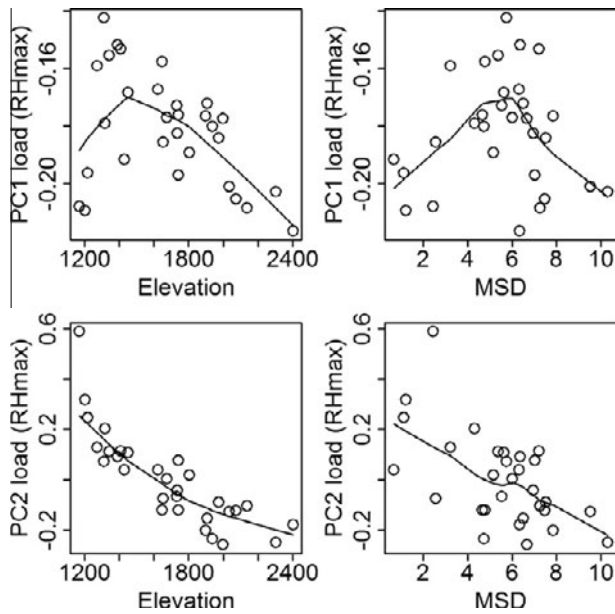


Fig. 6. Scatter plots and lowess smoothing curves showing relationships between PC loadings from maximum relative humidity, elevation and the multiscale dissection index (MSD).

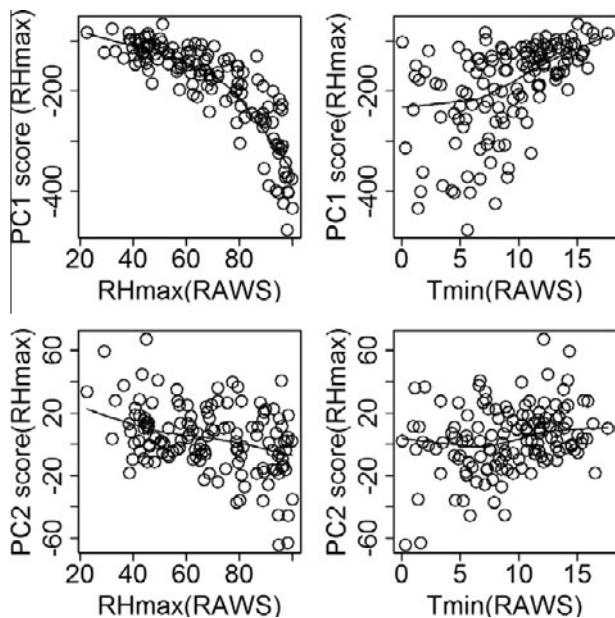


Fig. 7. Scatter plots and lowess smoothing curves showing relationships between PC loadings from maximum relative humidity and RAWs-observed maximum relative humidity and minimum temperature.

are shown in Fig. 9. Two divergent patterns are evident, one in the spring and early summer, and one in the fall. Early season (July) ERC values were as much as 100% lower on North-facing slopes than South-facing slopes at upper elevations, primarily as a result of delayed snowmelt timing (Fig. 9). Biweekly density plots of ERC values reveal similar patterns (Fig. 10). ERC is multi-modal across much of the fire season, with low and high peaks reflecting spatial variation with terrain. The distribution shifts toward higher ERC in September. At peak fire season (September 15–28), ERC becomes uni-modal, with most of the landscape shifted toward higher ERC. In the late season (August and September), nocturnal cold

air drainage and high relative humidity fostered fuel moisture recovery in valley bottoms, where fuel moistures and ERC values were 30% and 45% higher and lower, respectively at peak fire danger (September 29th). Dry fuel moistures and relatively high ERC values persisted on low elevation, South-facing slopes. The driest conditions were observed 100–200 m above the valley floor where mid-slope thermal belts frequently developed above areas of cold air pooling.

4. Discussion

Climatic and biophysical variability associated with topographic position leads to highly variable spatial and temporal patterns of fuel moistures and wildfire danger across the fire season. These patterns are currently ignored by wildfire danger forecasting models, but have real implications for fire behavior and wildfire danger modeling. Nocturnal cold air drainage has emerged as an important feature of climate in mountains that is not addressed by most temperature models (Geiger, 1966; Whiteman, 2000). Temperature and humidity are highly correlated, and colder air temperatures in valley bottoms are accompanied by higher relative humidity which together lead to higher fuel moistures. This pattern became pronounced as the dry season progressed, as dry atmospheric conditions fostered advection and cold air drainage. Cold air temperature and relatively moist air draining into valley bottoms would allow fuel moistures there to recover at night. As day length shortens, cold air drainage begins earlier and timing of inversion breakup is delayed (Whiteman, 1982) periods of nighttime cold air pooling lengthen, exacerbating the effects of cold air drainage on fuel moistures.

For decades, fire managers have been interpreting regional fire danger in the context of weather observations from local fire weather stations. As such, they have become familiar with the relationships between various fire danger indices, such as ERC, and the likelihood of a fire. It is therefore important to maintain consistency between fire danger calculated at RAWs stations and other estimates of fire danger variations across a landscape. The normalization procedures presented here ensured consistency between RAWs-calculated fire danger indices and their microclimate induced spatial variations. This extends a fire manager's experience with well-known indices with additional information about how these indices vary across the landscape. These methods ensure that the daily worst-case fire danger conditions across the landscape are always consistent with RAWs-calculated values. However, we only used a single weather station in this study to demonstrate this concept. Future work should provide a means to incorporate surface weather observations from multiple stations to provide the best depiction spatial variations in fire danger over complex terrain. Thousands of sensors are currently being distributed throughout USFS Region 1 (Montana and Idaho). Data from these sensors will provide a means for developing high-resolution climatologies and wildfire danger forecasting models for mountainous regions of the northwestern US.

This study illustrates a simple and inexpensive framework for collecting high spatial resolution information about site, watershed or landscape-scale topoclimatic variability. The networks of temperature and humidity sensors used in this study cost a total of approximately \$5500 dollars and would take one person approximately 2 months to deploy and retrieve. They yield a remarkable amount of information about topoclimatic variation in complex terrain. Potential products from these data include empirically-based air temperature models (Holden et al., 2011), and similar models for daytime and nighttime relative humidity and vapor pressure deficit. Such models can be linked to historical datasets, and show some potential for producing high-resolution future

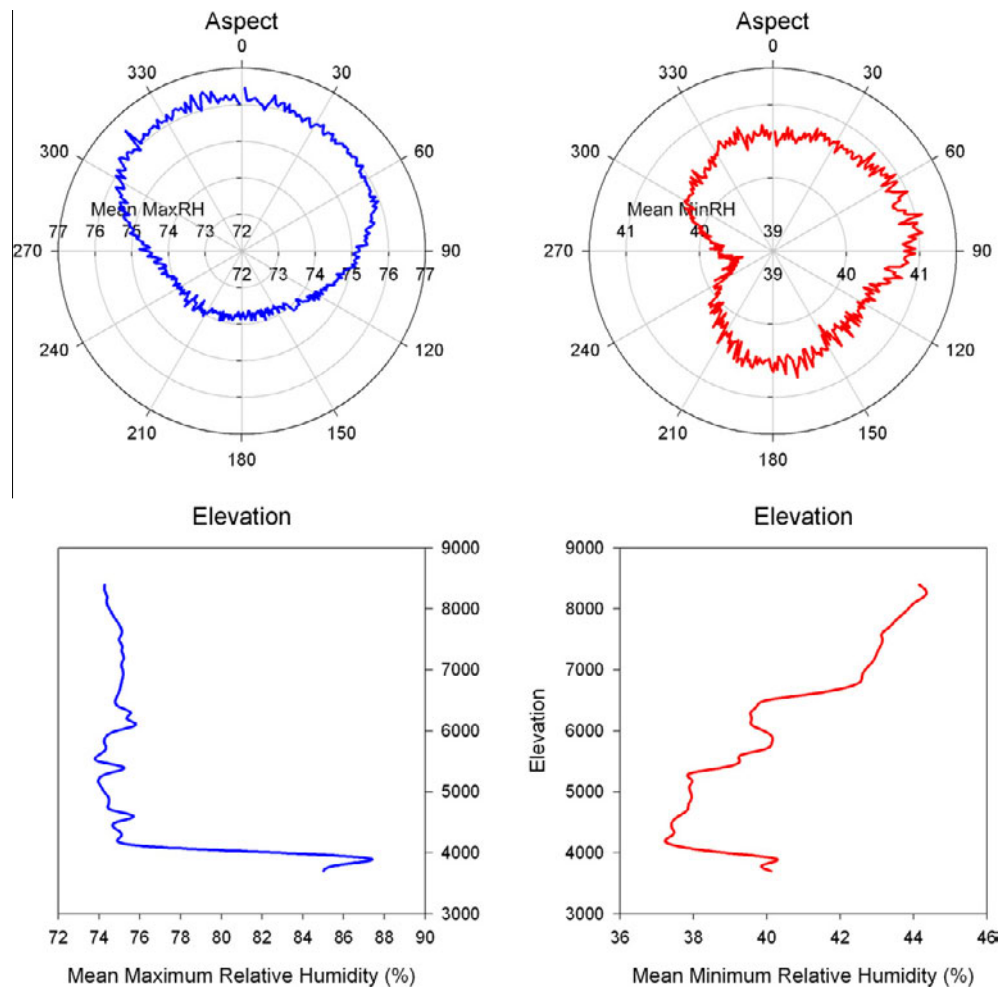


Fig. 8. Radial plots showing the distribution of maximum and minimum relative humidity by elevation and aspect.

climatologies based on the outputs from General Circulation Models (Holden et al., 2011).

The temperature and humidity models developed for this study demonstrate a simple, computationally efficient means of down-scaling climate to the scale of terrain. These models rely on predicted PC loading maps that are static spatial indices predicted to terrain variables. The fitted statistical models of PC1 and PC2 scores (time series) are stored in computer memory. These algorithms (A linear model for PC1 and a Random Forest model for PC2) could be loaded from memory and fit to either historical or real-time RAWS data and then applied back to the PC loading surfaces to produce daily high spatial resolution temperature and humidity surfaces. These models could be easily brought into operational use and to empirically correct RAWS in near real-time. Retrospective high-resolution climatologies could also be developed from RAWS or other gridded data sources and used to understand spatial and temporal patterns of historical wildfire danger at very fine resolutions.

Understanding the landscape patterns of remotely sensed burn severity has become an area of active research. A number of studies have demonstrated that topography significantly influences severe fire occurrence (Holden et al., 2009; Broncano and Retana, 2004; Bradstock et al., 2010; Lentile et al., 2006). However, these studies rely largely on topographic indices (elevation, aspect, dissection) that are indirect proxies for more physically-based variables. Relationships between elevation, solar radiation and surface air temperatures are well known. Additional morphometric indices show

potential utility for downscaling climatic and physical variables in complex terrain. For example, topographic dissection at multiple spatial scales appears to be correlated with snow ablation date. Snow drifting is an important component of snow accumulation and snowmelt (Tarboton and Luce, 1996). A 7×7 pixel (210×210 m) dissection index was a significant independent variable in our empirical snowmelt model. A multi-scale dissection index (Holden et al., 2011) was important for predicting both nocturnal air temperature and relative humidity. Similarly, a Topographic Position Index (TPI; Dylan et al., in review) was consistently an important predictor of burn severity occurrence. Continued development of empirical methods for resolving climatic and biophysical variation in complex terrain may rely on translation of these indices into models of physical variables.

Several studies have noted that climate and topography exert top down (synoptic atmospheric variation) and bottom-up (e.g. topography and vegetation) control on wildfire extent (Heyerdahl et al., 2001) and severity (Dylan et al., in review). Our analysis highlights the complex, fine-scale interactions between climate and topography that likely influence landscape-scale patterns of vegetation production, fuel conditions, fire occurrence, extent, behavior and ecological effects. Regionally synchronous fire years occur in the Northern Rockies during warm, dry springs (Morgan et al., 2008; Heyerdahl et al., 2008). Because our study was conducted during a single relatively cool, wet year, we can only speculate about how relative variation in fuel moisture patterns varies from year to year. Our results suggest a physical basis

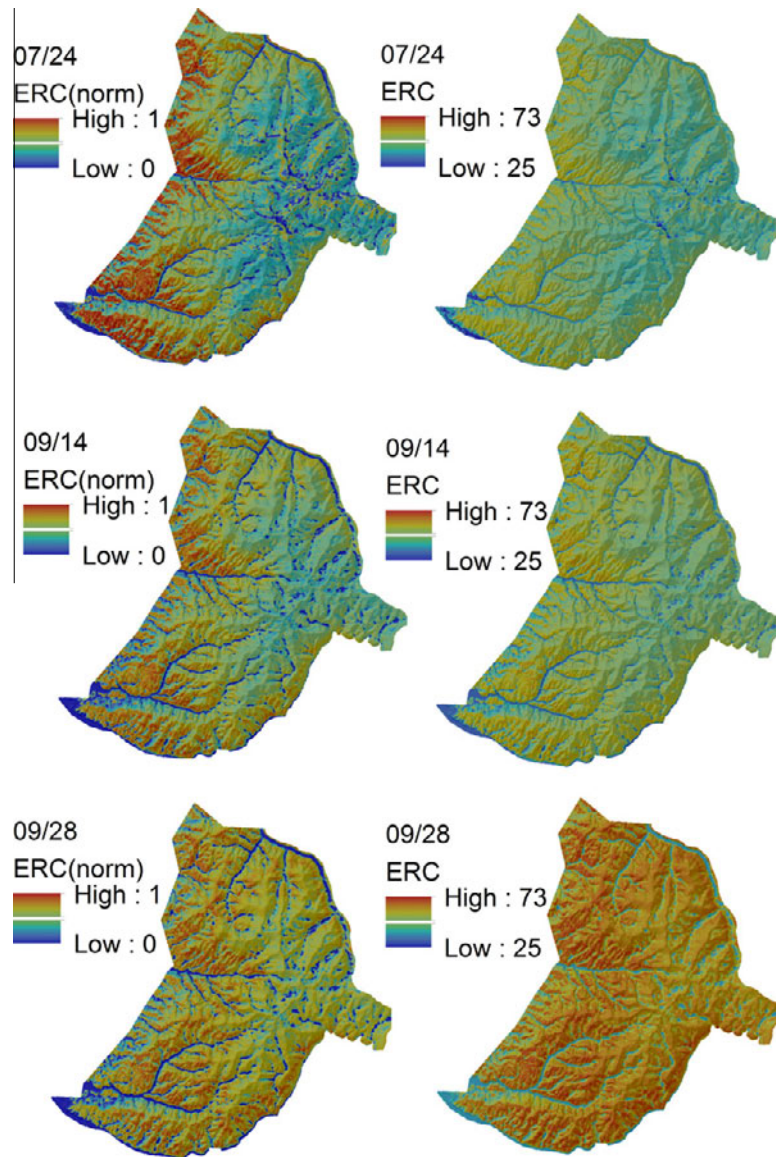


Fig. 9. Spatially-explicit predictions of the Energy Release Component for three example days during the study period: 24 July, 14 September and 28 September, 2009. The maps on the left show the Relative Fire Danger Index that has been normalized across its daily range of ERC values (Eq. (1)) and the maps in the right column show the final ERC values after the temporal fire danger trend from the RAWs station was added back to the grids (Eq. (2)).

behind climate–terrain interactions that could limit landscape-scale occurrence and spread of historical, naturally occurring wildland fires. Delayed snowmelt timing during cool springs would limit early season fire growth, while topo-climatic variation in the fall (cool, wet North slopes and valley bottoms) would also limit rate of spread, particularly during relatively cool, wet years. Additional analysis using historical reconstructions of high-resolution fire danger indices across multiple fire seasons would be needed to better understand this connection.

Wildfires, when viewed over a long enough time scale, are inevitable. They are also easier to suppress under cool, relatively wet conditions. Fire professionals face tremendous personal risk when making decisions about how to manage planned and unplanned wildland fires. It is not surprising then that most wildfires are suppressed before they become large and difficult to manage. This suppression paradigm continues despite the growing awareness of the vital ecological role, fire has always played in shaping many vegetation communities around the world (Agee, 1993). However, with continued fire management practices that favor initial attack and suppression, most of our total area burned

will continue to occur when wildfires that are ignited during extremely dry periods escape suppression, become large, and burn at high intensity. The severity of these fires, compared to those burning under more moderate conditions tends to be higher across a range of topographic conditions (Dylan et al., in review). In addition, these large fire incidents are more difficult to control, cost the public billions of dollars, and are dangerous to fight. Thus, by extinguishing fires that have the potential to become ecologically beneficial, we may be deferring some of the true “external” costs of landscape-scale fire management. This is particularly true in the western United States, where humans have expanded into and live in fire-prone, mountainous environments. Integration of fine-scale fuel moisture and potential energy release information into wildfire management decision making may be needed in order to make fully informed decisions about the risks and potential positive ecological effects of wildfires. Improved characterization of fine-scale wildfire fire danger and its application in fire management decisions could enhance firefighter safety, expand opportunities for fire use and potentially save the government millions of dollars.

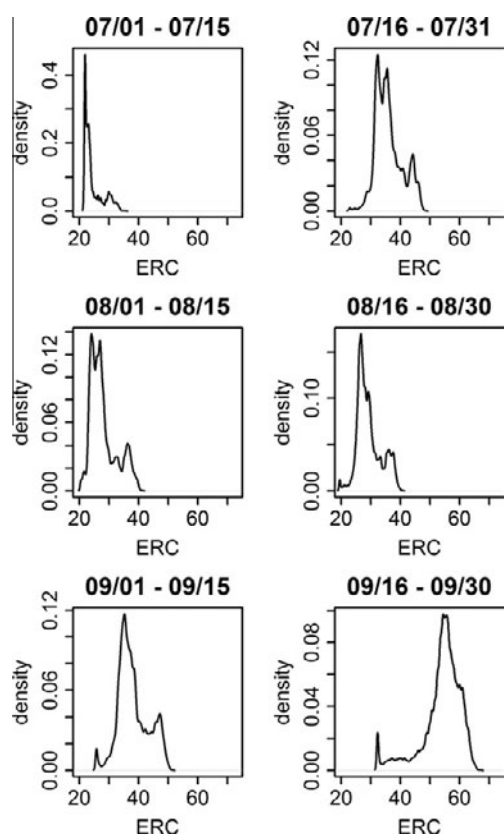


Fig. 10. Probability density plots of 2 week averaged ERC from July–September, 2009. Distributions are multi-modal and show a shift from most of the study area in low fire danger early in the season to the majority of the study area having high fire danger in the late season.

Despite growing concern about the potential ecological impacts of climate warming, vegetation management options for mitigating climate change impacts may be somewhat limited. Landscape-scale changes in vegetation are likely to be driven largely by disturbances such as insect and disease damage or wildfire. While insect and disease spread will be difficult or impossible to control, we do have some control over when and where wildland fires occur. Wildfires modify patterns of fuel and vegetation on the landscape which influence the severity of subsequent wildfires (Collins et al., 2009; Holden et al., 2010). By modeling the variation in fuel moistures and potential fire behavior at fine resolutions that are more consistent with fire as a physical process and incorporating that information into management decisions, we could potentially reduce the ecological risks associated with prescribed and wildland fire use. Improved understanding of climatic variation in complex topography and its influence on spatial variation in fire danger, fire behavior and post-fire ecological effects will likely be essential if we are to continue our efforts to help fire managers maintain and restore fire as a dominant and beneficial ecological process.

Acknowledgments

This work was funded and supported by Patti Koppenol and Bill Avey in USFS Region 1 fire management. This study was inspired in

part by George Weldon and Colin Hardy. The Missoula smokejumpers contributed to data collection that made this study possible. This work was completed in part by a NASA IDS grant to Jolly. Sam Cushman provided partial funding for sensors used in this study.

Appendix A. Supplementary data

Supplementary data associated with this article can be found, in the online version, at [doi:10.1016/j.foreco.2011.08.002](https://doi.org/10.1016/j.foreco.2011.08.002).

References

- Agee, J.K., 1993. Fire Ecology of Pacific Northwest Forests. Island Press.
- Andrews Patricia, L., Loftsgaarden Don, O., Bradshaw Larry, S., 2003. Evaluation of fire danger rating indexes using logistic regression and percentile analysis. *International Journal of Wildland Fire* 12, 213–226.
- Bradstock, R., Hammill, K., Collins, L., Price, O., 2010. Effects of weather, fuel and terrain on fire severity in topographically diverse landscapes of south-eastern Australia. *Landscape Ecology* 25, 607–619.
- Broncano, M.J., Retana, J., 2004. Topography and forest composition affecting the variability in fire severity and post-fire regeneration occurring after a large fire in the Mediterranean basin. *International Journal of Wildland Fire* 13, 209–216.
- Cohen, J., Deeming, J.E., 1985. The National Fire Danger Rating System: Basic Equations. In: USDA (Ed.), Pacific Southwest Forest and Range Experiment Station, p. 16.
- Collins, B.M., Miller, J.D., Thode, A., Van Wagtenonk, J.W., Stephens, S.L., 2009. Interactions among wildland fires in a long-established Sierra Nevada natural fire area. *Ecosystems* 12, 114–128.
- Dylan, G.K., Holden, Z.A., Morgan, P., Crimmins, M.C., Luce, C.H., Heyerdahl, E.K., submitted for publication. Both topography and climate affected forest and woodland burn severity in two broad regions of the western US, 1984 to 2006.
- Evans, I.S., 1972. General geomorphometry, derivatives of altitude and descriptive statistics. *Spatial Analysis in Geomorphology*. Harper and Row, New York, pp. 17–90.
- Geiger, R., 1966. *The Climate Near the Ground*. Harvard University Press.
- Gillespie, A., Abrams, M., Yamaguchi, Y., 2005. Scientific results from ASTER. *Remote Sensing of the Environment* 99, 1–220.
- Hastie, M., Tibshirani, S., 1990. *General Additive Models*. Chapman and Hall.
- Heyerdahl, E.K., Brubaker, L.B., Agee, J.K., 2001. Spatial controls of historical fire regimes: a multiscale example from the interior West, USA. *Ecology* 82, 660–678.
- Heyerdahl, E.K., Morgan, P., Riser, J.P., 2008. Multi-season climate synchronized historical fires in dry forests (1650–1900), Northern Rockies, USA. *Ecology* 89, 705–716.
- Holden, Z.A., Abatzoglou, J.T., Luce, C., Baggett, L.S., 2011. Empirical downscaling of minimum air temperature at very fine resolutions in complex terrain. *Agricultural and Forest Meteorology*.
- Holden, Z.A., Morgan, P., Evans, J.S., 2009. A predictive model of burn severity based on 20-year satellite-inferred burn severity data in a large southwestern US wilderness area. *Forest Ecology and Management* 258, 2399–2406.
- Holden, Z.A., Morgan, P., Hudak, A.T., 2010. Burn severity of areas reburned by wildfires in the Gila Wilderness. *New Mexico, USA. Fire Ecology*.
- Hubbart, J., Link, T., Campbell, C., Cobos, D., 2005. Evaluation of a low-cost temperature measurement system for environmental applications. *Hydrological Processes* 19, 1517–1523.
- Lentile, L.B., Smith, F.W., Shepperd, W.D., 2006. Influence of topography and forest structure on patterns of mixed severity fire in ponderosa pine forests of the South Dakota Black Hills, USA. *International Journal of Wildland Fire* 15, 557–566.
- McGaughey, R.J., 2010. FUSION/LDV: Software for LIDAR Data Analysis and Visualization. United States Department of Agriculture Forest Service Pacific Northwest Research Station.
- Morgan, P., Heyerdahl, E.K., Gibson, C., 2008. Multi-season climate synchronized widespread forest fires throughout the 20th century, Northern Rockies, USA. *Ecology* 89, 705–716.
- Tarboton, D.G., Luce, C., 1996. Utah Energy Balance Snow Accumulation and Melt Model (UEB) – Computer model technical description and user guide USDA Forest Service Research Technical Report.
- Whiteman, C., 2000. *Mountain Meteorology: fundamentals and applications*. Oxford University Press, New York.
- Whiteman, D.C., 1982. Breakup of temperature inversions in deep mountain valleys: part I. Observations. *Journal of Applied Meteorology* 21, 270–289.